AFRL-SR-BL-TR-00-

REPORT DOCUMENTATION PAGE

0024

1. AGENCY USE ONLY (Leave blank)	2. REPORT DATE	3. REPORT TYPE AND DATES COVERED
	21 January 2000	Final Report 15 June 1996 - 31 December 1999

4. TITLE AND SUBTITLE
(U)
(AASERT96) Response Enhancement for PITLIF Instrument

5. FUNDING NUMBERS
PE - 61103D
PF - 3484
SA - WS
G-F49620-96-1-0272

6. AUTHOR(S)
Galen B. King and Normand M. Laurendeau

7. PERFORMING ORGANIZATION NAME(S) AND ADDRESS(ES)
Purdue University
West Lafayette, IN 47907-1288

8. PERFORMING ORGANIZATION REPORT NUMBER

9. SPONSORING / MONITORING AGENCY NAME(S) AND ADDRESS(ES)
AFOSR/NA
801 North Randolph Street, Room 372
Arlington, VA 22203-1977

10. SPONSORING / MONITORING AGENCY REPORT NUMBER

11. SUPPLEMENTARY NOTES

12a. DISTRIBUTION / AVAILABILITY STATEMENT
Approved for public release; distribution is unlimited.

12b. DISTRIBUTION CODE

13. ABSTRACT ***(Maximum 200 Words)***

Previous work for AFOSR has demonstrated the feasibility of picosecond time-resolved laser-induced fluorescence (PITLIF) for real-time, quenching-corrected measurements of minor species concentrations in laminar and turbulent flames. Specifically, time-series measurements of CH and OH fluorescence have been demonstrated for the first time via PITLIF. These measurements can provide power spectral densities (PSDs) as well as the more traditional probability density functions (PDFs). However, the quenching rate coefficient must simultaneously be measured to quantify the fluorescence time series, and this was not previously accomplished. In this report, a new photon-counting procedure is presented that possesses the data processing rate required for quantitative concentration measurements on a time scale shorter than that characteristic of turbulence. This technique was first applied to laminar flames, and a correction procedure which accounts for the nonlinear response of the photon-counting system was derived for extension of the technique to turbulent flames. The fully developed PITLIF instrument was then applied to the first known measurements of quantitative OH time series in turbulent reacting jets.

14. SUBJECT TERMS
Laser-Induced Fluorescence, Picosecond Time-Resolved Laser-Induced Fluorescence (PITLIF)
Fluorescence decays

15. NUMBER OF PAGES
33

16. PRICE CODE

17. SECURITY CLASSIFICATION OF REPORT	18. SECURITY CLASSIFICATION OF THIS PAGE	19. SECURITY CLASSIFICATION OF ABSTRACT	20. LIMITATION OF ABSTRACT
Unclassified	Unclassified	Unclassified	UL

Response Enhancement for PITLIF Instrument

Final Report
Air Force Office of Scientific Research
Grant No. F49620-96-1-0272
September 1, 1996 - December 31, 1999

Galen B. King and Normand M. Laurendeau
School of Mechanical Engineering
Purdue University
West Lafayette, IN 47907-1288

ABSTRACT

Previous work for AFOSR has demonstrated the feasibility of picosecond time-resolved laser-induced fluorescence (PITLIF) for real-time, quenching-corrected measurements of minor species concentrations in laminar and turbulent flames. Specifically, time-series measurements of CH and OH fluorescence have been demonstrated for the first time via PITLIF. These measurements can provide power spectral densities (PSDs) as well as the more traditional probability density functions (PDFs). However, the quenching rate coefficient must simultaneously be measured to quantify the fluorescence time series, and this was not previously accomplished. In this report, a new photon-counting procedure is presented that possesses the data processing rate required for quantitative concentration measurements on a time scale shorter than that characteristic of turbulence. This technique was first applied to laminar flames, and a correction procedure which accounts for the nonlinear response of the photon-counting system was derived for extension of the technique to turbulent flames. The fully developed PITLIF instrument was then applied to the first known measurements of quantitative OH time series in turbulent reacting jets.

1 RESEARCH OBJECTIVES

Quantitative measurements of radical concentrations in flames are required for an understanding of important interactions between fluid mixing and chemical reactions (Drake and Pitz, 1985). Advances in laser-based techniques have made possible nonperturbing quantitative measurements of such species concentrations. In particular, laser-induced fluorescence (LIF) possesses both the spatial and temporal resolution necessary for monitoring radical concentrations in reacting flows (Barlow and Carter, 1994). Unfortunately, LIF usually suffers from an inverse dependence on the local quenching rate coefficient. Although laser-saturated fluorescence (LSF) permits measurements of species concentrations without recourse to quenching calculations (Reisel *et al.*, 1997), the LSF technique requires large laser powers which forces the laser repetition rate to be on the order of 10 Hz or less. This repetition rate can provide mean concentrations and probability density functions (PDFs), but it is clearly too slow to resolve species fluctuations in turbulent flames. High repetition rate lasers, on the other hand, can be utilized for measuring turbulent species fluctuations, but the quenching rate coefficient must be obtained within sampling times on the order of the Kolmogorov temporal scale, i.e., on-the-fly.

This research seeks to provide a technique which can quantitatively measure minor-species concentrations rapidly and continuously such that a time series of the fluctuating concentration can be recovered. These time series permit the computation of unique statistics such as the power spectral density (PSD) and supplement the information recovered from existing LIF techniques. Over the past four years, a new Ti-Sapphire laser system has been implemented to demonstrate, for the first time, rapid measurements of OH- and CH-fluorescence time series and subsequently the generation of both fluorescence PSDs and PDFs via picosecond time-resolved laser-induced fluorescence (PITLIF). However, the lack of a quenching correction did not permit the measurements to be quantitatively interpreted as minor-species concentrations.

In this final AASERT report, the development of a novel photon-counting instrument for PITLIF is presented. This equipment permits the correction of a fluorescence time series for variations in the electronic quenching coefficient on-the-fly so as to convert the fluorescence time series to a concentration time series. The theory, instrumentation, and implementation of this procedure is presented along with results for the hydroxyl radical in laminar flames. A correction procedure is next presented which was derived to account for nonlinearities in the photon-counting equipment. Using the complete PITLIF instrument with this correction procedure, measurements of the first known quantitative OH-concentration time series in a turbulent flame were obtained. The PSDs and PDFs determined from these time series are also presented and the unique nature of this measurement is discussed.

2 RESEARCH ACCOMPLISHMENTS

2.1 PITLIF Theory

By applying the radiative rate equations to a simple two-level model, the photon-counting data obtained from the improved PITLIF instrument can be shown to give a quenching-independent measurement of concentration. For PITLIF, a short laser pulse excites molecules from the ground level to an excited electronic level. It is assumed that all of the initial population is in the ground level before excitation, that the width of the laser pulse, Δt, is short compared to

the quenching time, and that the laser power is constant over the temporal width of the pulse. For sufficiently low laser power, the number density in the excited level immediately following the laser pulse, N_2^o(cm^{-3}), is given by

$$N_2^o = N_1^o W_{12} \Delta t \tag{1}$$

where N_1^o is the initial number density and W_{12} is the rate coefficient for stimulated absorption (s^{-1}). Following the laser pulse, the population of the excited level will decay to the ground level. In the absence of laser irradiation, absorption and stimulated emission can be neglected so that during the decay the number density of the excited level is given by

$$N_2(t) = N_1^o W_{12} \Delta t \exp(-t/\tau) \tag{2}$$

where τ is the excited state lifetime (s). The excited state lifetime is given in terms of the rate coefficient for spontaneous emission, A_{21}, and the quenching rate coefficient, Q_{21}, by

$$\tau = (A_{21} + Q_{21})^{-1}. \tag{3}$$

Thus, the measured temporal fluorescence signal is proportional to the instantaneous number density in the excited level. It also depends on the probe volume, V_c (cm^3), the solid collection angle, $\Omega/4\pi$, and the quantum efficiency of the detector, η. In addition, background radiation (say from flame chemiluminescence) provides a constant photon flux, B. Combining these terms, the time-dependent rate of photons incident on the detector (photons/second) is given by

$$S(t) = \eta(\Omega/4\pi) W_{12} \Delta t A_{21} V_c N_1^o \exp(-t/\tau) + B. \tag{4}$$

We have previously shown that PITLIF can be used to monitor the integrated fluorescence signal fluctuations on the time scale of turbulence (Renfro *et al.*, 1998) and that fluorescence lifetimes can be obtained in similar but separate experiments (Reichardt *et al.*, 1996). The primary accomplishment of the present research is an improvement to PITLIF, termed the laser-induced fluorescence triple integration method (LIFTIME), which measures only a portion of the total fluorescence signal given by Eq. (4)

LIFTIME utilizes three integrated areas beneath the fluorescence decay to determine the quenching rate coefficient (inverse of the fluorescence lifetime), the peak decay amplitude, and the fluorescence background. These three measurements are given by

$$D_2 = \int_{0.9ns}^{4.4ns} S(t)dt, \quad D_3 = \int_{4.4ns}^{7.9ns} S(t)dt, \quad D_4 = \int_{7.9ns}^{11.4ns} S(t)dt \tag{5}$$

where D_2, D_3, and D_4 are integrated photon counts from a gated photon counting system. These bins are schematically shown in Fig. 1. The limits of integration of these bins were chosen to improve the sensitivity of the PITLIF system based on the experimental work to be described in this report. In practice, the number of photons arriving at the detector in each of these bins is much less than one for a single laser pulse; thus, the integrated bins must also be averaged over many laser cycles. In addition to these gated bins, a fourth ungated photon-counting measurement, D_1, permits determination of the total fluorescence signal, i.e.,

$$D_1 = \int_0^\infty S(t)dt = C_f N_1^o \tau + (B/L) \tag{6}$$

where C_f is a calibration constant and L is the laser repetition rate. LIFTIME is modeled after the Rapid Lifetime Determination (RLD) method of Ballew and Demas (1989). The RLD method determines the peak decay amplitude and fluorescence lifetime by calculating the ratio of two integrated areas under the fluorescence decay. LIFTIME improves upon the RLD method by adding a third integrated bin capable of directly monitoring the background, which can be a

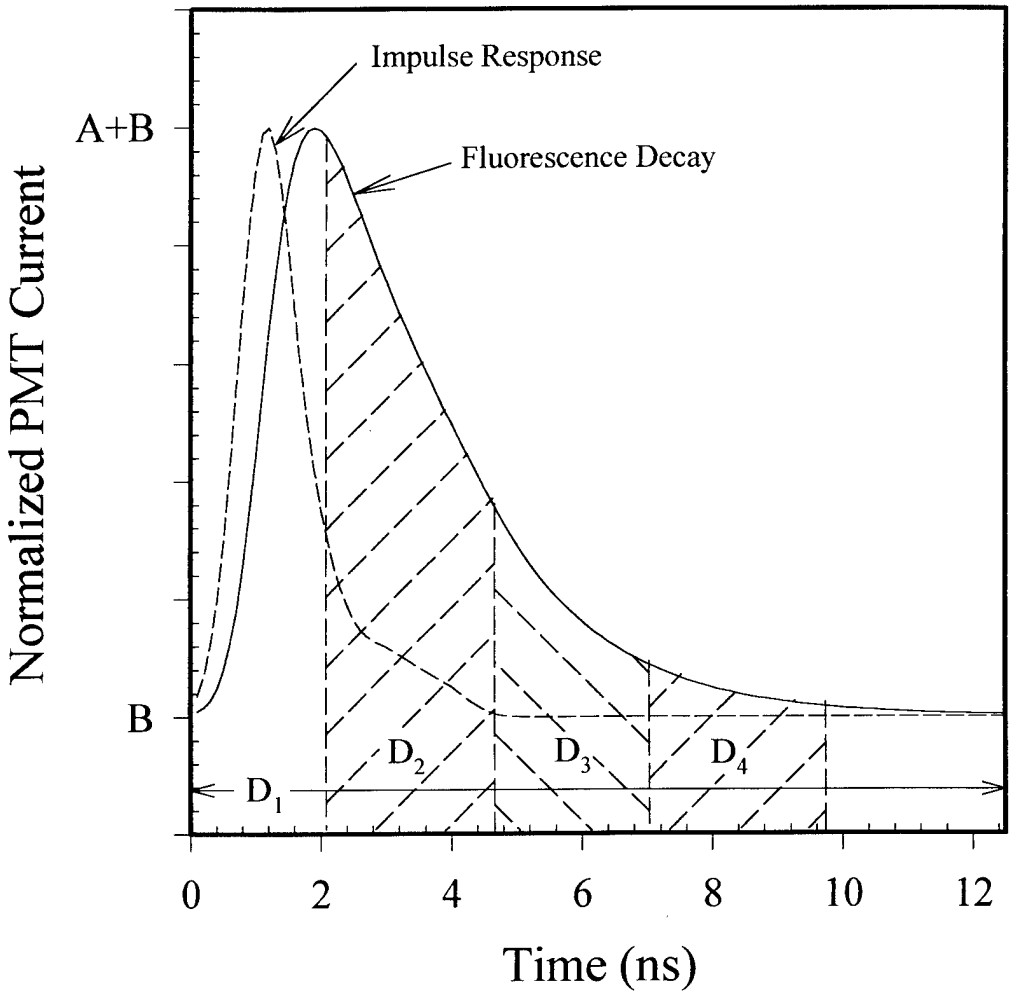

Figure 1. Graphical representation of the LIFTIME method. D_1 is 12.5 ns wide, whereas D_2, D_3, and D_4 are fixed at 3.5 ns. The dashed line is the impulse response of the PITLIF system. The background, *B*, is typical of flame emission, and the amplitude, *A*, is proportional to concentration.

significant source of signal from flames. For the conditions given by Eq. (5) the fluorescence lifetime and background can be found from

$$\tau = \frac{\Delta t}{\ln[(D_2 - D_3)/(D_3 - D_4)]} \tag{7}$$

$$B = \frac{D_2 C^2 - D_4}{\Delta t (C^2 - 1)} \tag{8}$$

where Δt is the width of each integrated bin (3.5 ns in this case) and $C = \exp(-\Delta t/\tau)$. These equations can be derived by neglecting the instrumentation response from the PMT and by assuming that the background is constant (i.e., not correlated with the laser pulse). Invoking these assumptions, the relationship among the three areas is $(D_4\text{-}B\Delta t) = (D_3\text{-}B\Delta t)C = (D_2\text{-}B\Delta t)C^2$, which easily leads to Eqs. (7) and (8).

In summary, if simultaneous time series of integrated photon counts (given by Eq. 4) can be measured, then the lifetime and flame emission background can be determined from Eqs. (7) and (8). These values can be used to correct the total fluorescence signal from Eq. (6) to quantitatively determine the ground-state concentration, N_1^o.

2.2 Experimental Setup and Procedure

A diagram of the laser system including the burner station is shown in Fig. 2. A Spectra Physics Tsunami, regeneratively mode-locked, Ti:Sapphire laser (80-MHz repetition rate) was pumped by a 20-W, Spectra Physics argon-ion, multi-mode laser. For the hydroxyl measurements to be presented, the resulting IR beam was frequency tripled to ~309 nm in a CSK SuperTripler. The output beam was recollimated by two UV lenses and focused by a 22.9-cm focal length, 5.1-cm diameter UV lens to form the probe volume above the burner assembly. For the tripled beam, the beam diameter (e^{-2}) was measured at the probe volume to be ~71 μm in two perpendicular directions. The laser power was approximately 18-24 mW which resulted in an average probe volume irradiance of $\sim 3.5\times10^5$ mW/cm^2. The $Q_1(8)$ transition of the (0,0) vibronic band (309.33 nm) of OH was chosen for excitation. This line displays an approximately ±5% Boltzmann fraction variation over the temperature range 1500-2250 K.

The hydroxyl fluorescence was collected at a 90-degree angle from the incident laser beam by two 14.1-cm focal length, 10.2-cm diameter UV lenses with a magnification of 4.1. This allowed collection of approximately 1/15 of all fluorescence photons emitted from the probe volume. The wavelength of the measured fluorescence was selected by use of a 0.25-m monochromator. An adjustable slit at the entrance to the monochromator allowed the probe volume in the flame to be limited along the beam path. The beam diameter itself defines the other two probe-volume dimensions, although black tape on the monochromator was used to limit some flame emission in the axial direction. These probe-volume settings were varied throughout the measurements to control the total signal level. For most measurements, the spectral window was set at a total bandwidth of 10 nm centered at 309 nm. A Hamamatsu HS5321 PMT detected the fluorescence at the exit plane of the monochromator. The PMT was biased at -2500 V to increase the single-photon pulse height for subsequent leading-edge discrimination. This PMT has a risetime of 700 ps and a transit time spread of 160 ps. The PMT impulse response function (~1 ns FWHM) is also shown in Fig. 1 and is compared to a typical fluorescence decay and the gated photon-counting measurements of PITLIF.

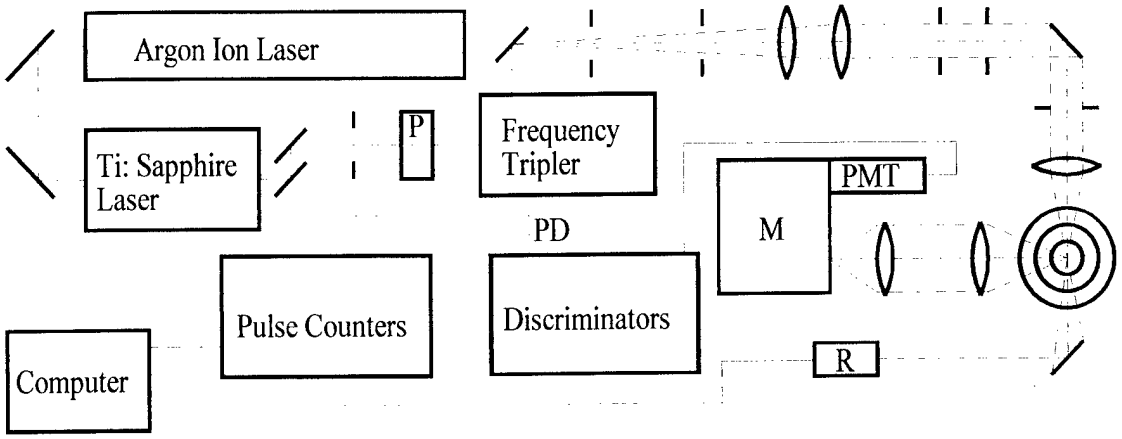

Figure 2. Experimental setup for the laser system: P, polarization rotator; M, 0.25-m monochromator; R, radiometer; PD, photodiode trigger from the laser to the discriminators.

The detailed wire schematic for the gated, photon-counting system is shown in Fig. 3. Briefly, the system consists of two LeCroy model 4608C, eight-channel discriminators connected to four EG&G Ortec logic-pulse counting boards. Several channels on the first discriminator are used to convert each PMT pulse into four logic (NIM) pulses and to convert each pulse from a photodiode (PD) in the Ti:Sapphire cavity to a 9-ns NIM pulse. The laser PD pulse acts as the logical inverse of the desired gate and forces the gates to be locked to the arrival time of the laser pulse. All of the channels of the second discriminator are simultaneously inhibited by the PD NIM pulse and are used to gate three of the four PMT NIM pulses (D_2-D_4). This second discriminator takes the place of a double-balanced mixer, which is common to many gated, photon-counting systems, and only permits output pulses in the absence of the PD NIM pulse. Unlike many other gated, photon-counting systems, the gates for LIFTIME are fixed in time (relative to the laser pulse). Separate cable delays for each of the three PMT inputs to the second discriminator ensure that each gate passes the appropriate portion of the fluorescence decay. The ungated PMT NIM pulse from the first discriminator and the three outputs from the gated discriminator are separately counted by the four EG&G pulse counters shown schematically in Fig. 3. These comprise the measured bins D_1-D_4 of Fig. 1. The four photon-counting boards each have an 8192 channel memory and can be sampled simultaneously. Each channel acquires counts over many thousands of laser pulses as set in software. The maximum sampling rate (channel advance rate) for the boards is 500 kHz, well above that needed for turbulence studies.

To demonstrate the feasibility of LIFTIME, two known fluorescence mediums, diphenyloxazole (PPO) and quinine sulfate monohydrate (QSM), were employed. PPO was chosen because its fluorescence lifetime represents a standard of 1.28 ns (Lampert *et al.*, 1983). QSM was chosen as its lifetime can be varied through dilution in salt solutions (O'Conner *et al.*, 1982). Seven solutions of QSM were created with decay constants ranging from 1.0 to 3.0 ns. Calibration was effected by employing a digital signal analyzer (DSA) and a calibrated convolute-and-compare technique previously used with the PITLIF instrument (Reichardt *et al.*, 1995). This standard technique has been shown to provide correct decay constants with less than 10 percent error at the 95% confidence level (Reichardt *et al.*, 1996).

Figure 4 is the resulting calibration plot for LIFTIME as expressed with respect to the DSA measurements. As expected, the instrumentation causes the measured decay constant to be slightly larger than the actual decay constant. This is especially true for the higher lifetimes. Nevertheless, a linear fit can be constructed which effectively corrects for the slight instrumentation errors produced by the photon-counting system. An interesting feature of the comparison in Fig. 4 is the relative error between the two techniques. The DSA has an uncertainty of about 3 percent, whereas that for the LIFTIME system is less than 1 percent (95 percent confidence level) at a sampling rate of 1 Hz.

2.3 PITLIF Measurements of Hydroxyl at Low Signal Levels

For simplicity, premixed laminar flames were chosen for the first application of LIFTIME to combustion systems. In particular, three $CH_4/O_2/N_2$ premixed flat flames (ϕ = 0.6, 0.8, 1.0) were created using a 6.1-cm McKenna burner with a molar N_2/O_2 dilution ratio of 3.1. The hydroxyl concentration at each flame position was measured by employing LIFTIME for 10 seconds at a sampling rate of 1 Hz. The approximate probe volume was 57 μm x 71 μm x 15 μm. This probe volume was chosen by monitoring the signal from the PMT for the ϕ = 0.8 flame and

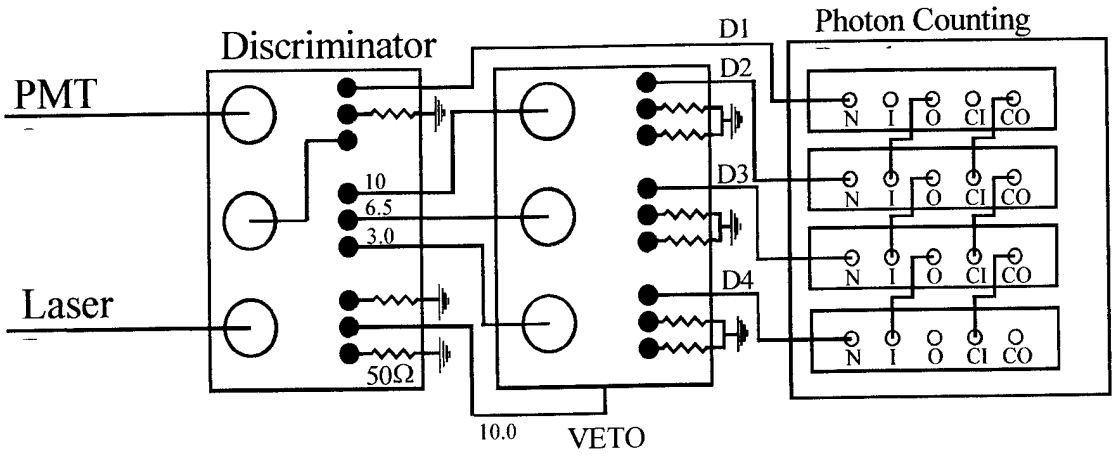

Figure 3. Wire schematic for the LIFTIME system. N's, NIM inputs from the discriminator; I, start signal input; O's, start signal outputs; CI's, channel advance inputs; CO's, channel advance outputs; PD, photodiode. Unused signals are 50-Ω terminated, and 10.0, 6.5, and 3.0 ns represent the delays placed in the respective lines.

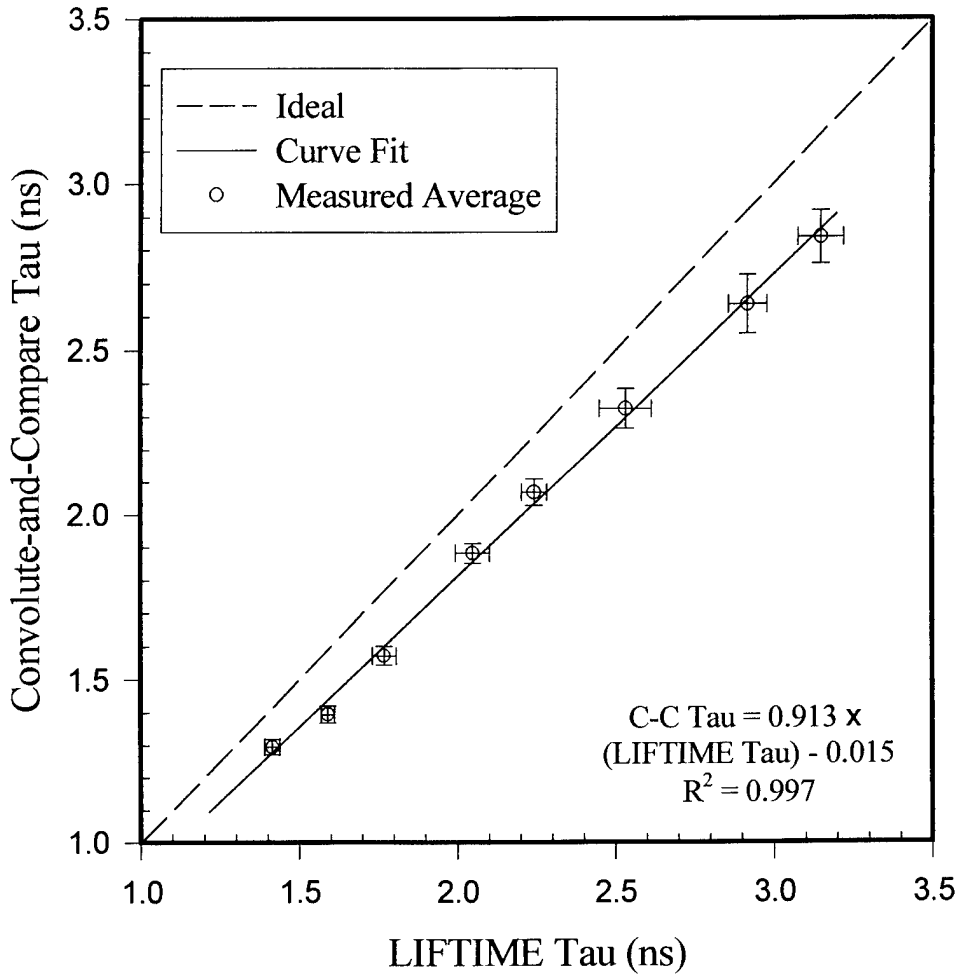

Figure 4. Calibration of LIFTIME with convolute-and-compare (C-C) algorithm by use of a DSA. Error bars are at the 95% confidence interval and include uncertainties caused by temperature fluctuations in the laboratory.

closing the entrance slit on the 0.25-m monochromator until the signal dropped below 400,000 photons per second. This resulted in an average of 200 laser pulses per photon which ensured negligible photon pulse pileup in the LIFTIME system (O'Conner and Phillips, 1984).

The OH concentration was calibrated via a simple ratio at two measured locations, using the following equation:

$$C_{OH} = \frac{(D_1 - B)C^*_{OH}\tau^* P^*}{(D_1^* - B^*)\tau P} \tag{8}$$

where C_{OH} is the concentration at a unknown point and C^*_{OH} is the concentration at a known calibration point. The parameters D_1, B, τ, and P represent the measured signal, background signal, fluorescence lifetime, and laser power at the unknown point and the asterisk indicates the same parameters at the calibration point. Thus, to determine accurate number densities, an established calibration point is needed. The Sandia one-dimensional flame code PREMIX (Kee *et al.*, 1985), when using the GRI 2.11 kinetic mechanism (Bowman *et al.*, 1995), was used to predict the OH concentration in the ϕ = 0.8 methane flame at 6 mm above the burner surface. This prediction was used as the concentration at the calibration point. All measured concentrations in other flat flames are based on this prediction and the LIFTIME measured fluorescence signal, background signal, fluorescence lifetime, and laser power at the calibration point. The justification for this procedure is based upon the findings of Reisel *et al.* (1997), who showed that the GRI 2.11 mechanism gave excellent agreement with laser-saturated fluorescence measurements in similar lean premixed ethane flames. We have verified that both lean ethane and methane flames give equivalent calibrations.

Figure 5 shows the axial hydroxyl profiles obtained for the three methane flames in comparison to the results calculated via PREMIX (Kee *et al.*, 1985) and the GRI 2.11 mechanism (Bowman *et al.*, 1995). From Fig. 5, we observe that the measured OH concentrations agree very well (within 7%) with the predicted concentrations. The largest difference is observed for the ϕ = 1.0 measurements, which is consistently low in comparison with the model. This difference is likely due to the uncertainty in the equivalence ratio, since the OH concentration will decrease if the flow rates are slightly incorrect either in the rich or lean direction. The error bars for the OH concentrations shown in Fig. 5 are based on five different error sources. The five error sources are statistical variations, laser position uncertainty, laser wavelength fluctuations, fuel flow uncertainties, and instrumentation changes owing to temperature fluctuations in the laboratory. The statistical uncertainty in the fluorescence lifetime owing to shot noise was the minimum source of error for a 1-Hz sampling rate. The largest source of error stemmed from flow rate uncertainties, which was approximately 7% for flames with $\phi \geq 1.0$.

The LIFTIME system was further verified by measuring hydroxyl concentrations in five premixed ethane flames and in a laminar counterflow diffusion flame (Pack *et al.*, 1999). The ethane flames were used to demonstrate LIFTIME measurements of OH concentration in rich flames, which had a much lower signal-to-background ratio (SBR) than the lean methane flames. The flow rate and dilution ratio for these flames were chosen to permit comparisons with previous LSF measurements obtained by Reisel *et al.* (1997). Additional measurements in a laminar counterflow diffusion flame were used to demonstrate LIFTIME's ability to accurately measure fluorescence lifetimes and species concentrations when the lifetime varies throughout a flame (Pack *et al.*, 1999). As for the previous measurements, each of these additional flames was calibrated to a known methane premixed flame (ϕ = 0.8). The measured OH concentrations in the

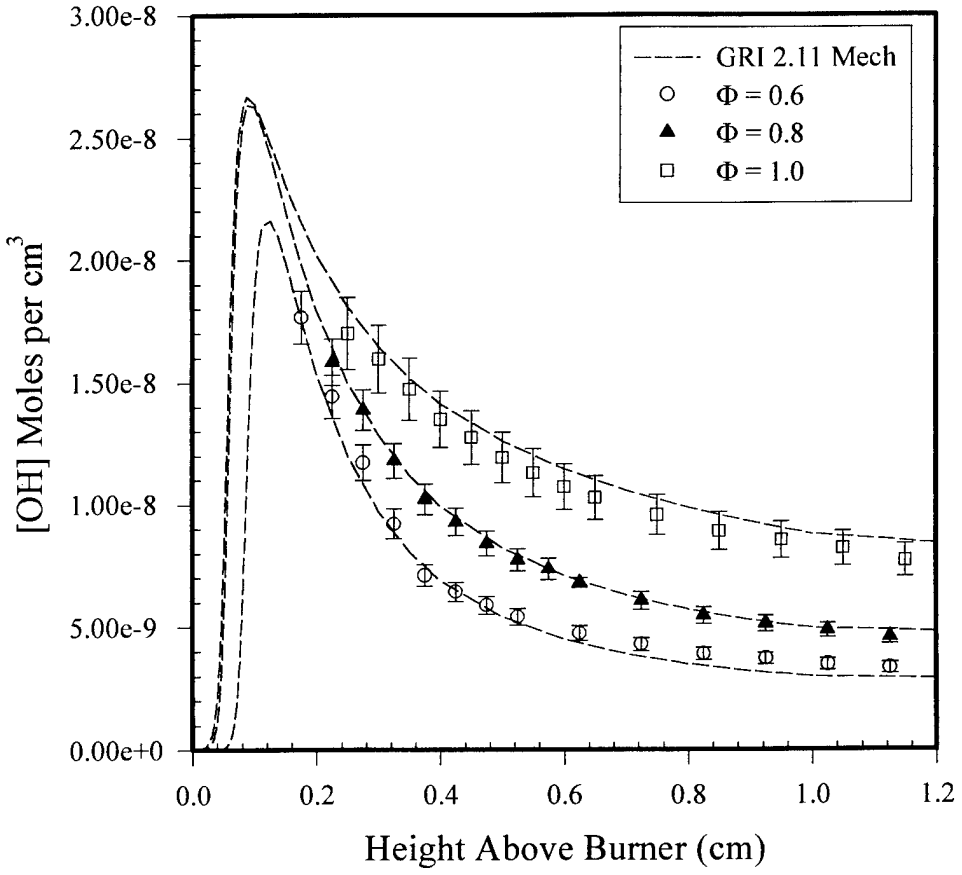

Figure 5. Measured hydroxyl concentrations in $CH_4/O_2/N_2$ flames. Error bars are based upon a 95% confidence interval of the mean. The measurements are compared to predicted results using the GRI 2.11 mechanism. The 0.6-cm point at $\phi = 0.8$ is the calibration point used for all flames.

ethane flames showed good agreement (within 15%) with previous LSF measurements; similarly, all measurements in the counterflow flame agreed well (within 10%) with GRI 2.11 predictions when applying the OPPDIFF code (Lutz *et al.*, 1996).

To this point, LIFTIME has been shown to provide accurate hydroxyl concentrations in laminar premixed and diffusion flames, even for an unknown emissive background. In general, hydroxyl concentrations can be determined within ten seconds for laminar flames with a statistical uncertainty less that 10%. LIFTIME has also been shown to generally provide fluorescence lifetime measurements in such flames with less than 5% uncertainty. If lifetime variations are not considered, either experimentally or computationally, measured concentrations can be in error by as much as 29%. By increasing the measured fluorescence signal, quantitative hydroxyl concentration measurements at higher sampling rates should be possible in turbulent flames; however, higher fluorescence signals cause photon pulse pileup so that a suitable correction procedure must be developed for this saturation process.

2.4 PITLIF Measurements of Hydroxyl at High Signal Levels

The hydroxyl measurements in laminar flames discussed above were purposively limited to low sampling rates (<500 Hz) owing to the need to attenuate the fluorescence signal below that level for which pulse pileup becomes important. For such low signals, the response of the photon-counting system remains linear; however, shot noise limits the maximum frequency resolution. At the high sampling rates needed for turbulent flames, however, the gated photon-counting technique clearly requires a pulse-pileup correction procedure. This analytical routine has recently been developed by Renfro *et al.* (1999a), and has been shown to provide reliable fluorescence decay amplitudes, lifetimes, and backgrounds at data collection rates up to 35 million photoelectrons per second. For the Ti:Sapphire laser system, this collection rate represents an average of almost one detected photon per two laser pulses. This limit results from photomultiplier tube (PMT) saturation and is not necessarily a limitation of the LIFTIME system, although operation much above 35 million counts per second is doubtful without substantial improvements to present pulse-discriminator technology.

The requirement for a correction procedure that accounts for photon saturation is based on the following scenario. Upon receiving an analog pulse which meets the threshold criterion, the discriminator begins to output a NIM logic pulse (0 to -0.8 V, typically less than 5 ns duration, with ~1 ns rise and fall times). However, if a second acceptable analog pulse arrives during the time required to complete the NIM pulse output, the discriminator is unable to respond (or is dead) and the measured count rate will be lower than the actual incoming pulse rate. For the LeCroy discriminators, the minimum dual-pulse resolution (DPR) is 4.5 ns based on the manufacturer's specifications. Fortunately, the output pulse rate of the PITLIF system is directly related to (although not linear with) the input pulse rate; hence, a one-to-one relationship can be derived such that the measured output rate can be used to infer the actual input rate.

The resulting iterative procedure, termed "saturate-and-compare", is similar to convolute-and-compare routines which are commonly used to evaluate instrumentation response functions for accurate determinations of fluorescence lifetimes. The general procedure is as follows: (1) assume values for the decay parameters (τ, B, and A); (2) simulate a perfect decay; (3) saturate the decay based on the observed behavior of the PITLIF system; (4) compute the simulated bin counts, D_2-D_4; and (5) compare the simulated and measured counts to improve the decay

parameters, eventually converging to the correct values. While the mathematical procedure is quite complicated (Renfro *et al.*, 1999a), the general scheme is based on simply fitting the measured photoelectron count rate to an exponential array so as to represent the fluorescence decay. The decay array is then saturated according to the following two assumptions: (1) all photon statistics are governed by the Poisson distribution, and (2) once a photon is counted, no more photons may be counted for a period of time equal to the dual-pulse resolution.

As verification of the upgraded system's capabilities, measurements were retaken using PPO and each of six quinine sulfate monohydrate (QSM) solutions. A calibration plot of the saturate-and-compare results as compared to the known values determined via convolute-and-compare is shown in Fig. 6. The experimental lifetimes are almost identical to the low-signal LIFTIME results of Pack *et al.* (1998). Moreover, the statistical error in fluorescence lifetime (68% confidence interval) remains below ±10% up to a sampling rate of 7.8 kHz, a considerable improvement over the previous 500-Hz limit for unsaturated photon counting. Thus, the saturate-and-compare routine is providing the correct average lifetime from 1.3 to 3.0 ns at sampling rates exceeding 4 kHz. The error bars in Fig. 6 show the standard deviation measured over the full range of signal and signal-to-background (SBR) levels. The relatively small size of the error bars indicates that the system can converge to the correct solution over all of the expected input conditions.

Since the ultimate goal of the PITLIF technique is to provide concentration time-series, the effects of experimental and numerical uncertainty on the measured concentration is of more direct importance than the effects on the fluorescence lifetime. Moreover, the absence of a substantial background for liquid solutions does not adequately simulate actual conditions that are encountered in hydroxyl measurements (Gaskey *et al.*, 1990). Hence, to further verify the pulse-pileup correction procedure, measurements of OH concentration and lifetime were obtained in the previous methane calibration flame (ϕ=0.8). The measurements were made with a SBR ($(D_2-D_4)/D_4$) of 2.6; furthermore, the concentrations were determined from the peak decay amplitude. The uncertainty in lifetime was very similar to that of PPO. However, the sampling rate at which the peak amplitude (or concentration) reached an error of ±10% was only 3.4 kHz, which is still a significant improvement over previous unsaturated work but unfortunately much less than that for the fluorescence lifetime. This is not unexpected, however, as the concentration requires indirect corrections for both the background and fluorescence lifetime, and thus involves more usage of shot-noise limited bin counts.

Figure 7 shows the average lifetime and concentration determined at a specific sampling rate of 5 kHz for various signal levels in the same CH_4 premixed flame. The measured concentration is scaled by the total signal level at each point such that it should be constant in the absence of saturation. Using the saturate-and-compare algorithm, the same lifetime (within ±0.5%) and concentration (within ±2.6%) are recovered regardless of the degree of saturation. For comparison, these same parameters were computed using Eq. (7) via the method (LIFTIME) described by Pack *et al.* (1998) which does not consider saturation. The need for the saturation correction is very apparent as the resulting error in lifetime exceeds 30% at the highest signal level, resulting in a 20% bias error in the computed concentration. The slight curvature that exists in the corrected lifetimes and concentrations as a function of fluorescence signal most likely arises from the change in SBR as the monochromator slit is opened and closed for this measurement. For each of the above measurements, the variation in average lifetime is always less than 2% over the full range of signal levels.

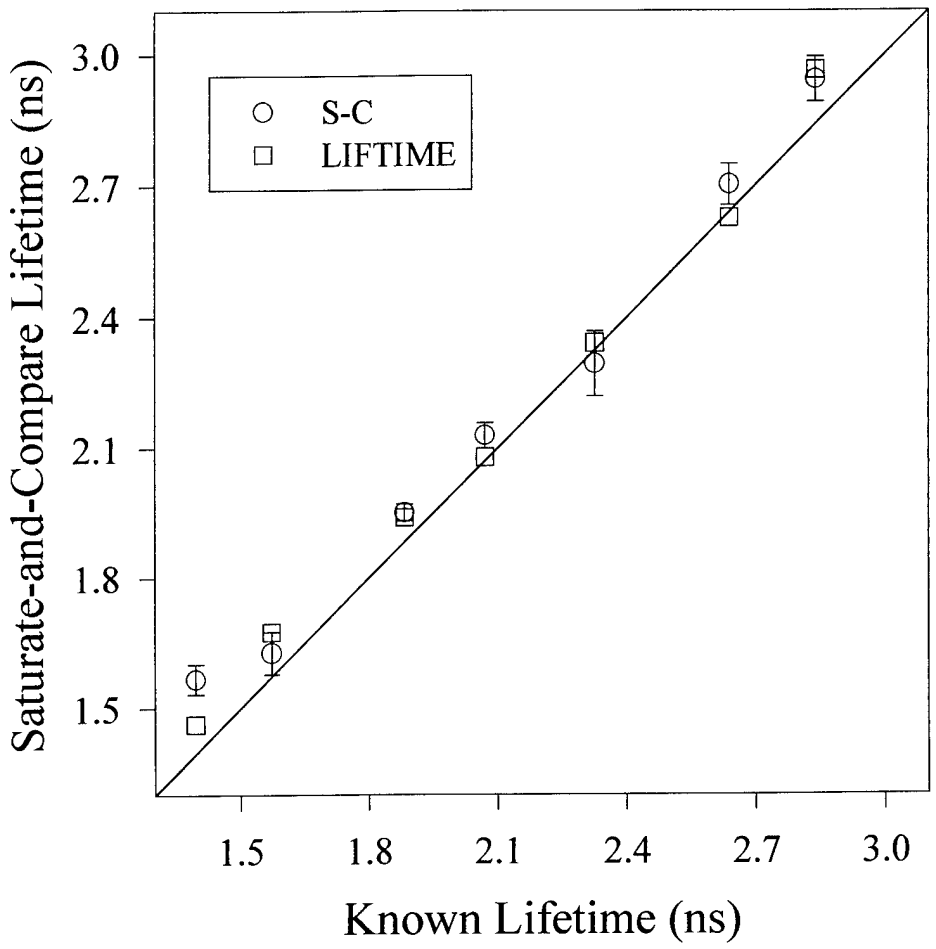

Figure 6. Calibration plot of saturate-and-compare (S-C) lifetimes as compared to the known convolute-and-compare measurements of Pack *et al.* (1998). Error bars represent the standard deviation (68% confidence interval) for measurements at many different signal levels and SBRs. The LIFTIME measurements from Pack *et al.* (1998) represent the exact solution at low signal levels.

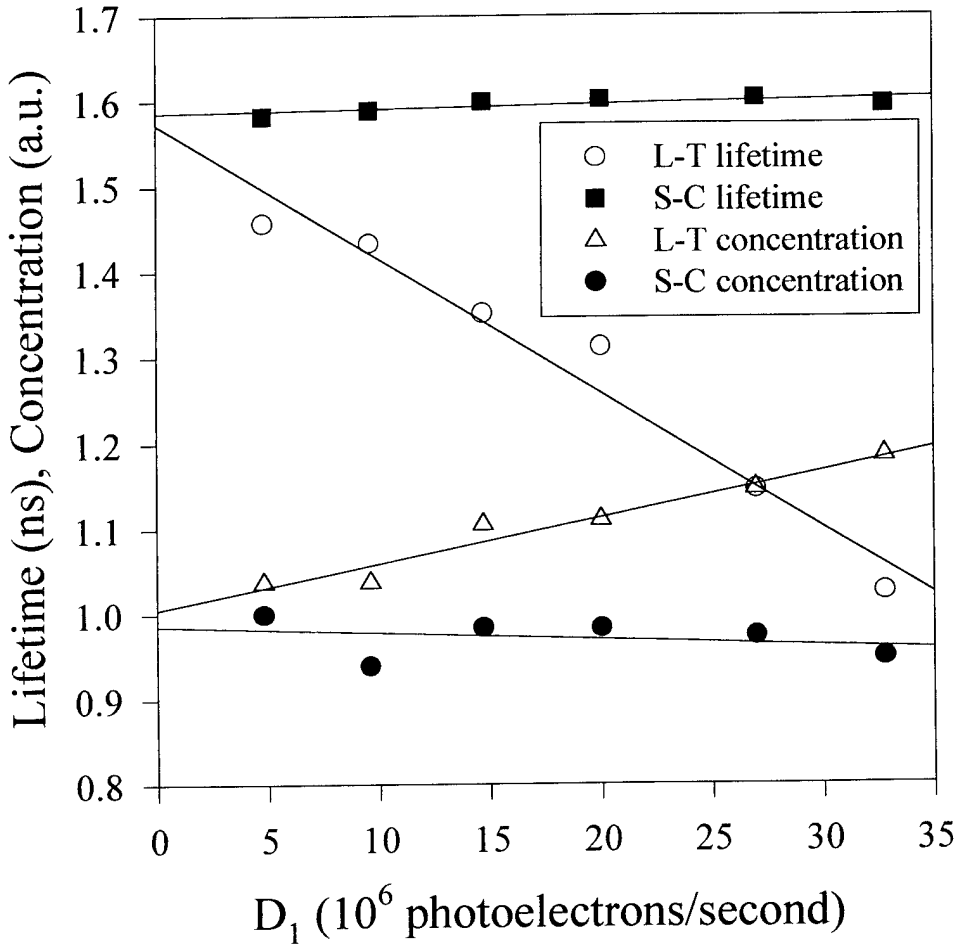

Figure 7. Lifetime and concentration versus signal (D_1) for measurements in a laminar premixed methane flame ($\Phi = 0.8$, $z = 3$ mm). The sampling rate is 5 kHz. The signal is varied by adjusting the monochromator entrance slit. The solution obtained via the saturate-and-compare (S-C) algorithm is compared with that obtained via LIFTIME (L-T) by neglecting saturation (Pack *et al.*, 1999). For both methods, the measured concentration is scaled by the total signal such that the results should be constant in the absence of saturation.

The low-signal measurements of Pack *et al.* (1999) were shown to yield excellent agreement with modeling and also with previous LSF measurements in a series of laminar, premixed ethane flames (Reisel *et al.*, 1997). As further verification of the accuracy of the saturate-and-compare algorithm, many of these previous measurements were repeated at higher signal levels. Figure 8 shows axial profiles of OH concentration in these same laminar, premixed, $C_2H_6/N_2/O_2$ flames. The dilution ratio for each flame was 3.1 and the equivalence ratio was varied from 0.6 to 1.6. All measurements were taken with a spatial resolution of ~250 μm along the laser beam. The peak signal corresponded to ~24 million photoelectrons/second. Each flame in Fig. 8 was calibrated against the 6-mm measurement in the ϕ=0.8 flame. The previous LSF measurements are shown for comparison (Reisel *et al.*, 1997). The agreement is excellent for nearly all cases. In particular, the PITLIF measurements resolve most of the peak locations and concentrations with high accuracy.

Additional measurements of hydroxyl concentration in a counterflow methane/air diffusion flame (25% fuel-side nitrogen dilution, overall flame stretch rate = 19.1 s^{-1}) are shown in Fig. 9. The burner is identical to that used by Ravikrishna and Laurendeau (1998) for NO measurements and the flow conditions are identical to those used by Pack *et al.* (1999) for OH measurements. As observed in Fig. 9, the present measurements, at a peak signal of 26 million photoelectrons/second and a sampling rate of 1 Hz, agree very well with the low-signal measurements from the previous work. Three data sets are shown for the saturation-corrected results in Fig. 9. One data set is computed from D_1 plus the measured background and lifetime, as $[OH] \propto (D_1-B)/\tau$. The other two curves are simply the amplitude, A, as determined from the saturate-and-compare routine. As observed, there is no discernable difference among the three evaluations of the hydroxyl concentration. This is expected on the basis of the rate equations governing the linear fluorescence technique (Reichardt *et al.*, 1996). Hence, for all remaining measurements in this report, the concentration has been determined directly from the peak amplitude of the fluorescence signal.

Finally, to confirm the efficacy of the saturate-and-compare routine at high sampling rates, additional measurements were obtained in a buoyant, laminar methane jet diffusion flame (Re = 70, burner diameter = 5.5 mm). Figure 10 shows a radial profile of both the OH concentration and lifetime in this flame at an axial height of 5 mm. Since this flame had a strong 15-Hz frequency corresponding to buoyancy-induced pulsations, the base sampling rate was extended to 100 Hz to avoid errors in the average lifetime measurements. These measurements were then repeated at a higher sampling rate of 4 kHz. At the location of peak concentration, the accuracy in concentration is ±10.4% including the uncertainties arising from calibration, which was again performed with respect to a $CH_4/N_2/O_2$ flame at ϕ=0.8.

In this section, the development of a saturation-correction scheme for application to gated photon counting measurements has been discussed in reasonable detail (Renfro *et al.*, 1999a). This analytically based routine has been shown to yield the same fluorescence lifetimes for liquid samples of diphenyloxazole and quinine sulfate monohydrate as those from previous unsaturated measurements obtained by Pack *et al.* (1999). The technique was then extended to hydroxyl measurements at higher sampling rates of 1-100 Hz in laminar premixed, laminar counterflow diffusion, and laminar jet diffusion flames. In each case, the results match either previous LSF measurements or LIFTIME measurements taken at lower photon count rates. Thus, the saturate-and-compare algorithm has been shown to be sufficiently robust for applications to a large range of practical flames over a wide range of signal levels and SBRs. Measurements in the laminar jet

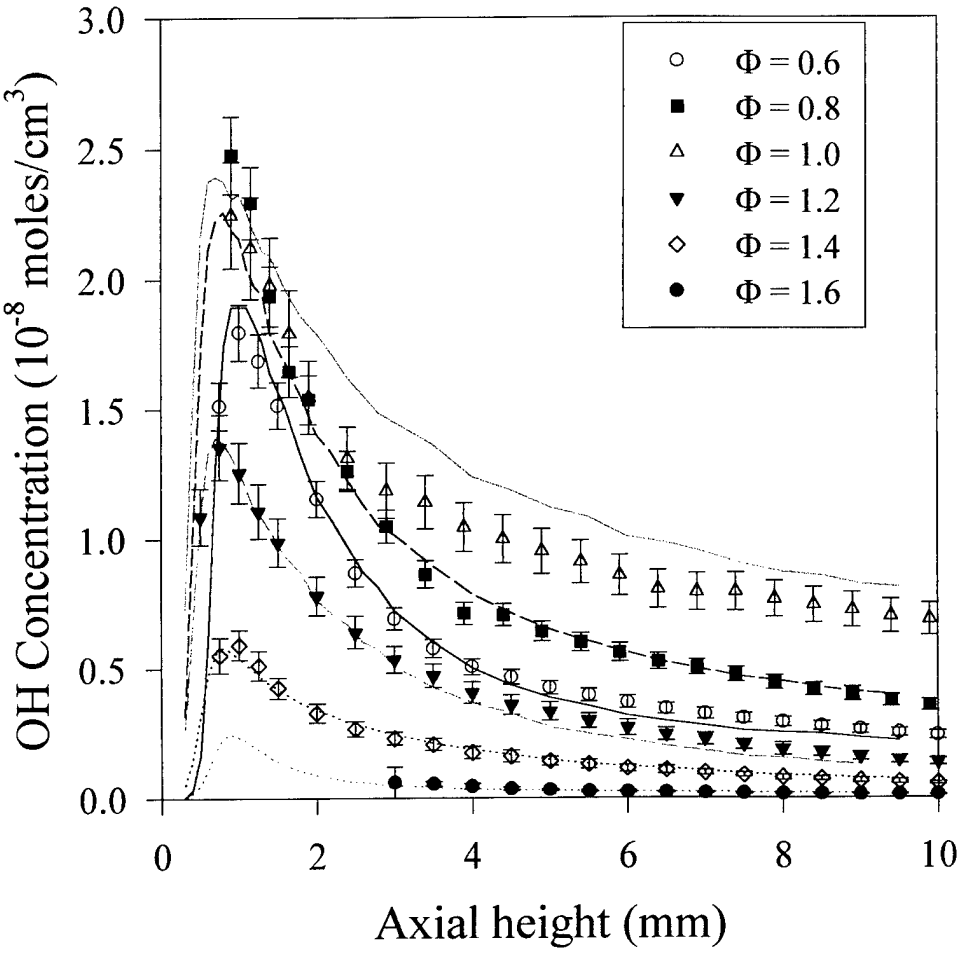

Figure 8. Measurements of OH concentration in six premixed ethane flames. The curves are the LSF data of Reisel *et al.* (1997). All measurements are calibrated to that at an axial height of 6 mm in the $\Phi = 0.8$ flame. Each point is the average of 10 measurements taken at a sampling rate of 10 Hz. The error bars represent the total accuracy (95% confidence interval) and include shot-noise, flow-rate errors, calibration errors, and temperature-fluctuation errors.

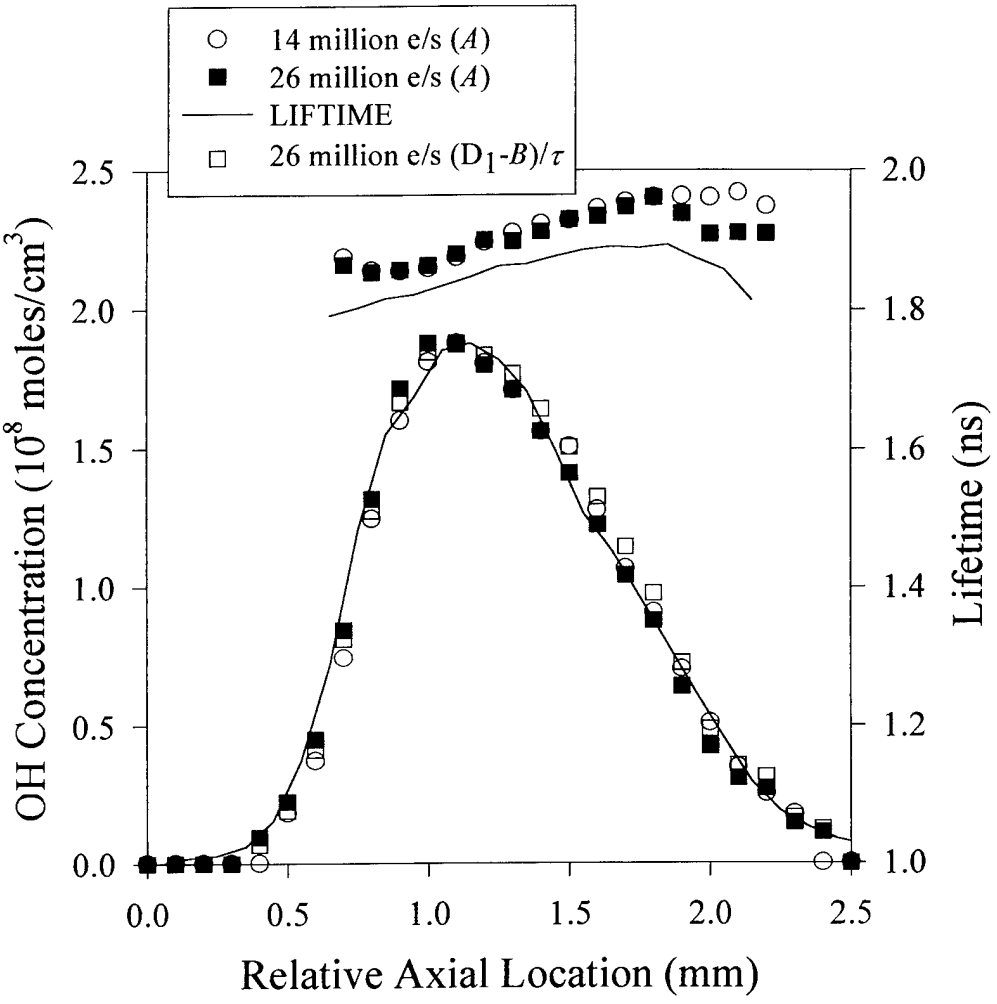

Figure 9. Comparison of hydroxyl measurements in a counterflow diffusion flame at high signal to those of Pack *et al.* (1999) at low signal. The sampling rate for these measurements was 1 Hz. Two signal levels are shown for the saturate-and-compare measurements. For the higher signal case, the concentration is computed both from the amplitude, A, and from D_1, plus B and τ, for comparison. The spatial resolution for this measurement is ~1 mm along the laser beam.

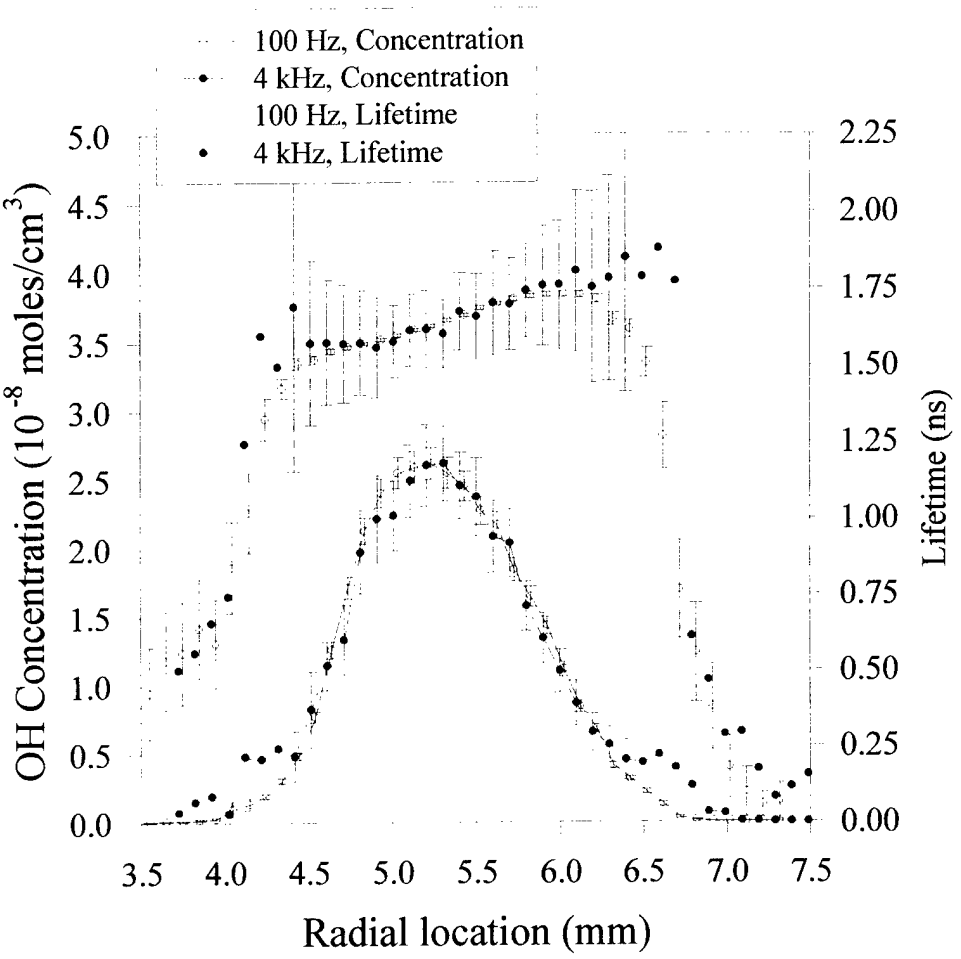

Figure 10. Measurements of OH concentration in a buoyant, laminar methane jet diffusion flame. The concentration error bars include repeatability, plus temperature and calibration errors, while the lifetime error bars consider only repeatability. For the 100 Hz measurements and 1 s of averaging time, the error bars represent the 95% confidence interval of the mean. For the 4 kHz measurements, the error bars represent the 68% confidence interval for single-point measurements.

diffusion flame were further extended to a sampling rate of 4 kHz and were found to agree with measurements obtained at a lower sampling rate while displaying a statistical uncertainty of ~10%. Hence, a sampling rate of ~4 kHz should provide sufficient accuracy for studies of the power spectral density in turbulent nonpremixed flames.

2.5 PITLIF Measurements of OH in Turbulent Nonpremixed H_2/Ar Flames

The previous improvements to PITLIF permit rapid simultaneous measurements of the fluorescence signal and lifetime, which can now be combined to determine a quantitative concentration time series for turbulent flames. From the measured time series, the temporal autocorrelation function and its Fourier transform, the power spectral density (PSD), can be recovered in addition to the more common PDF. In this section, the first quantitative hydroxyl PSDs from within a turbulent flame (Renfro *et al.,* 1999b) are presented. For these initial measurements, a series of turbulent H_2/Ar/air flames were employed so as to optimize the hydroxyl signal and thus ensure the reliability of the time series describing fluctuations in OH concentration. The quenching-corrected fluorescence measurements are again calibrated against a $CH_4/O_2/N_2$ (ϕ=0.8) premixed flat flame. This premixed flame was studied extensively by Pack *et al.* (1999) using the PITLIF technique, and the OH predictions were found to agree with the OH measurements to within 2%. Since the PITLIF technique directly considers the fluorescence lifetime in determining species concentrations, any variation in major-species concentrations and temperature from the $CH_4/O_2/N_2$ premixed to the H_2/Ar/air nonpremixed flames is an insignificant source of error in the calibration.

Time-series measurements of hydroxyl concentrations were made at five axial locations in five Ar-diluted, H_2/air nonpremixed flames ([Ar]/[H_2]=0.282). The Reynolds numbers based on room-temperature exit conditions for a 5.5-mm diameter burner were 2800, 5000, 9000, 13,000, and 17,000. At each height, measurements were made at many radial positions across the peak [OH] location. These fluorescence and lifetime time-series measurements were taken at a sampling rate of 4 kHz. Fifty one-second time series at each location were analyzed to obtain clean statistics. The measured data were converted to concentrations by specifically accounting for photon pulse pile-up in the detection system (Renfro *et al.,* 1999a). The resulting quantitative OH-concentration time series were then used to compute the PDFs and PSDs. The PSD is a Fourier-transform pair to the temporal autocorrelation function; thus, these two statistics provide the same temporal information, but in different forms (Box and Jenkins, 1976).

Figure 11 shows the measured radial profiles of [OH] and fluorescence lifetime in the Re=9000, H_2/Ar diffusion flame. In these flames, the lifetime is determined almost exclusively by the local temperature and water concentration. The lifetime changes from the air side to the fuel side of the [OH] peak low in the flame are due, primarily, to changes in water concentration across the OH peak. Higher in the flame, little change occurs in the lifetime over the spatial range where substantial OH is found. At these downstream locations, the temperature and water concentration change more gradually with distance from the flame centerline, leading to the observed lifetime trends. For measurements of mean [OH], the lifetime correction is significant as the average lifetime at x/D=2 is 12% higher than that at x/D=20 and the maximum lifetime in the flame is 43% higher than the minimum lifetime.

Previous minor-species time-series measurements (Renfro *et al.*, 1998) did not consider the effects of fluctuations in the fluorescence lifetime, which can now be directly investigated.

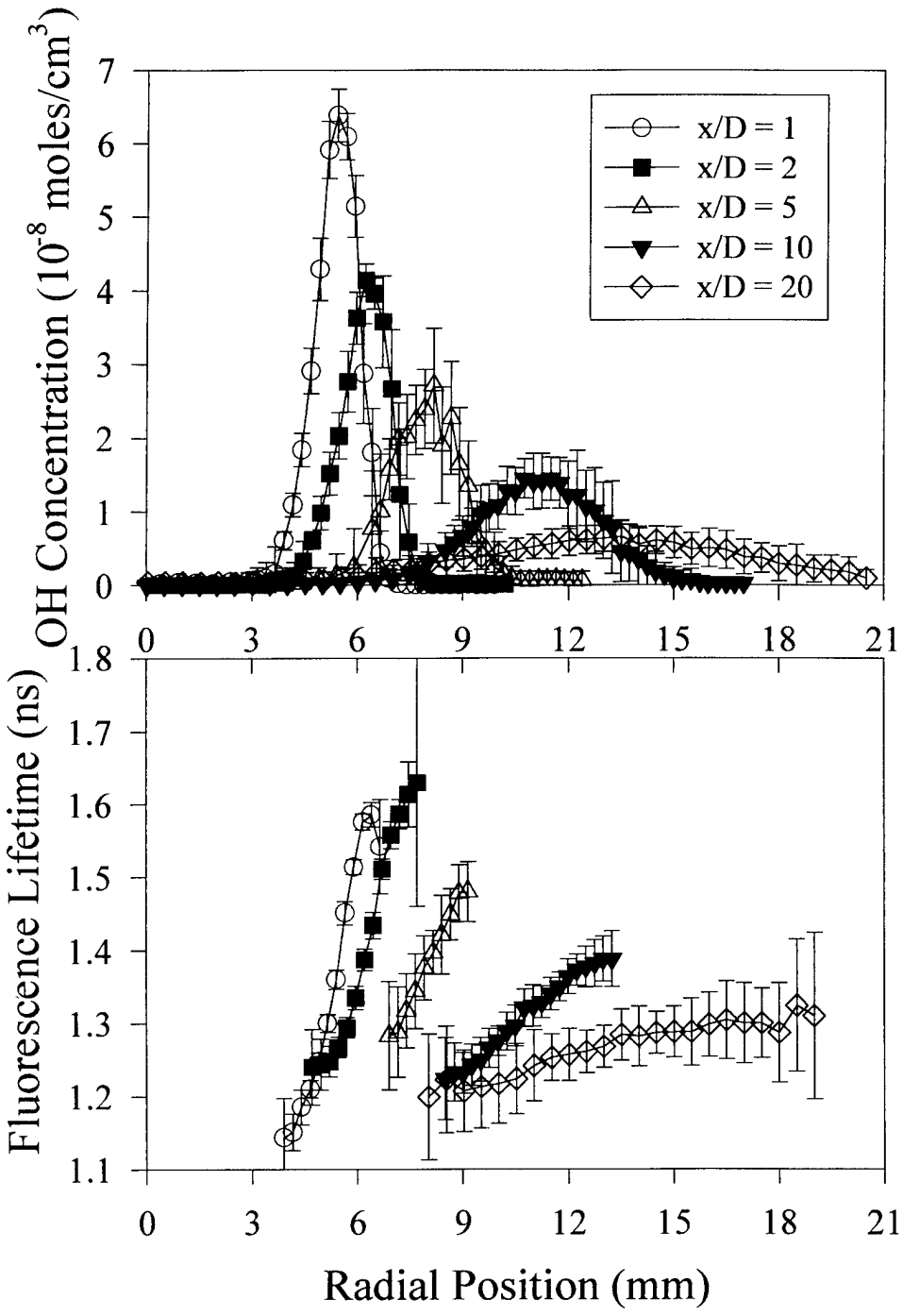

Figure 11. Radial profiles of OH concentration and fluorescence lifetime in the Re=5000 H_2/Ar flame. Error bars represent the repeatability of the measurement (95% confidence interval).

Figure 12 shows a comparison of concentration PSDs (corrected for lifetime) to uncorrected fluorescence PSDs in the Re=13,000 H_2/Ar flame. As observed, there is no difference in the concentration and fluorescence PSDs, indicating that the lifetime measurements are relatively unimportant to accurate determination of the frequency content of the concentration fluctuations. Each measurement location in each of the present flames was examined and each showed a similar comparison as that of Fig. 12. This independence can arise if the statistical weight of the lifetime fluctuations is small such that concentration fluctuations dominate the fluorescence time series. For OH measurements, the local gradient of the lifetime profile (Fig. 11) is much less than that of the concentration profile. Thus, as fluctuations cause the probe volume to sample different portions of the radial [OH] distribution, the concentration time series will contain more intense fluctuations than the lifetime time series. The measured fluorescence time series will then reflect these stronger concentration fluctuations.

Figure 13 shows the measured PSDs as a function of Reynolds number in each of the H_2/Ar/air flames. The relative energy in the PSDs at low frequencies decreases as the Reynolds number increases. Likewise, the relative energy at high frequencies increases and the high-frequency slope becomes less steep. These trends with increasing Reynolds number are similar to the trends that are observed in a single flame when going from the ambient air stream to the more turbulent fuel stream, but to a greater degree. This evolution versus Reynolds number is apparent at each axial height and radial location. Thus, it appears that the Reynolds number dominates the shape of the hydroxyl PSD in each of these H_2/Ar flames.

The limited literature available on the nature of PSDs in turbulent jets and nonpremixed flames indicates that the PSD for velocity in a homogenous, nonreacting, isothermal flow at $Re > 10^4$ generally decays with a log-log slope of -5/3 in the so-called inertial region (Tennekes and Lumley, 1972). This fundamental result is based on the assumption that the turbulent energy from large-scale fluctuations at the so-called integral scale cascades without loss of energy to smaller and smaller scales, with dissipation eventually becoming significant at the smallest scale in the flow, the so-called Kolmogorov scale. Since for most gaseous turbulent flows, the Kolmogorov length and time scales are approximately 500 μm and 100 μs, respectively (Daily, 1976), PITLIF time series can generally be measured at conditions equivalent to or superior to both of these minimum scales. Hence, PSDs derived from PITLIF time series are able to consider all of the temporal scales of importance to turbulent nonpremixed flames. Consequently, a key issue is the extent to which the -5/3 slope in the inertial subrange for velocity PSDs translates to a similar slope for important scalars of the flow field.

In general, most LDV studies in non-reacting jet flows at $Re > 10^4$ display a PSD slope close to the classical value of -5/3 through the inertial subrange. However, as the Reynolds number becomes much smaller, turbulence theory no longer predicts a -5/3 slope for velocity. Mydlarski and Warhaft (1996), for example, found that the PSD slope increased asymptotically from approximately -1.2 to -1.7 as the Taylor-microscale Reynolds number was raised from 50 to 473 in a grid-generated turbulent wind tunnel. This is a significant finding with respect to turbulent nonpremixed combustion owing to the strong effect of temperature on the kinematic viscosity. From this dependence, the Reynolds number will decrease by a factor of ~30 from room to flame temperatures. Thus, even for a relatively high Reynolds number based on the cold fuel flow rate, a -5/3 slope in the inertial subrange may not be encountered in a combustion environment. In fact, Gökalp et al. (1988) showed that the slope of the velocity PSD in a turbulent premixed flame is sometimes significantly higher and sometimes significantly lower than

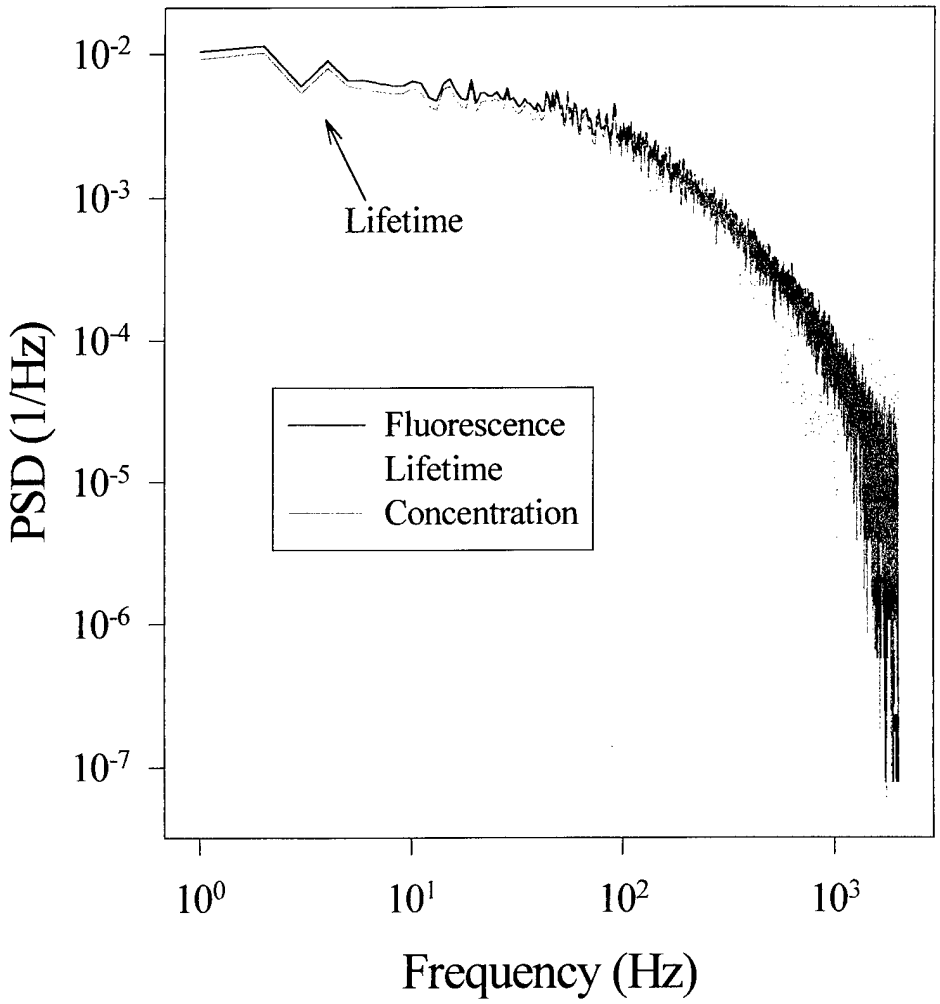

Figure 12. PSDs measured at x/D=5, 1-mm to the air side of the radial [OH] peak in the Re=13,000 H_2/Ar flame.

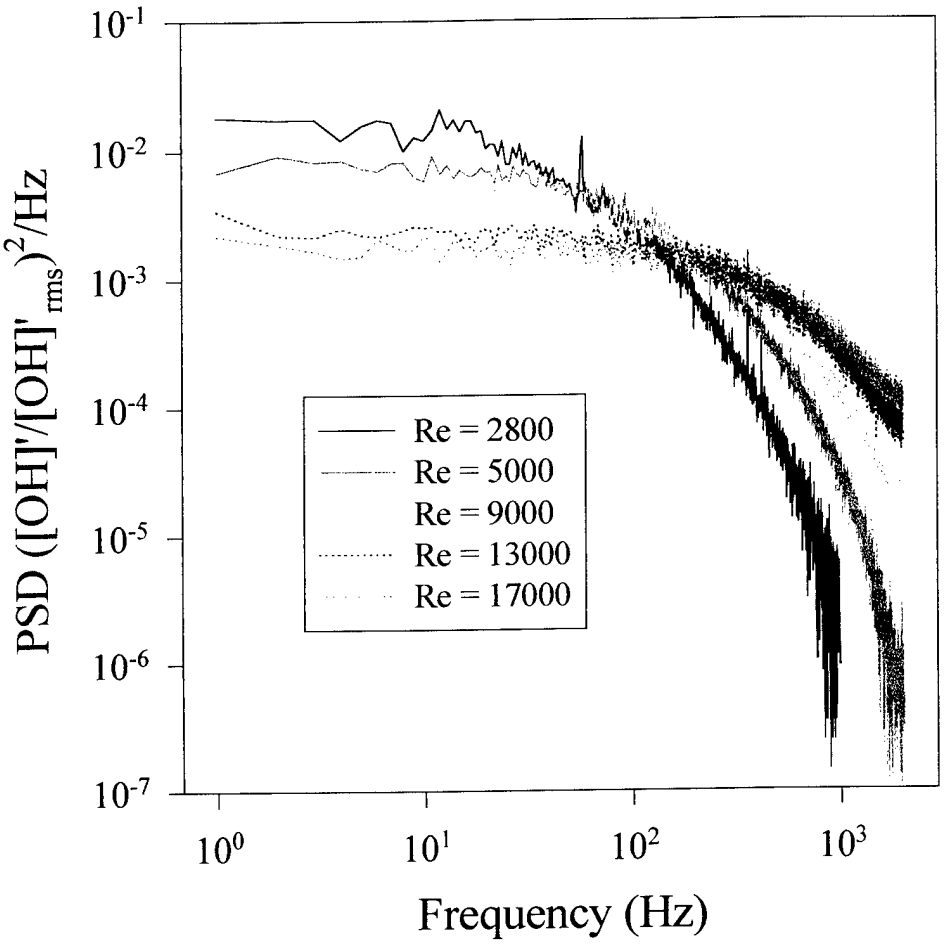

Figure 13. PSDs measured at x/D=20 at the radial location of peak [OH] in the H_2/Ar flames.

-5/3, thus indicating that flame behavior is much more complicated than can be understood from a simple viscosity effect. Because of this complication, Gökalp et al. (1988) proposed that interactions between velocity and scalar fluctuations complicate the velocity PSD, thus requiring measurements of both in order to understand the behavior of either PSD.

Measurements of concentration fluctuations in non-reacting jets by Miller and Dimotakis (1996) show that the PSD slope becomes steeper as the Reynolds number increases up to 72,000; however, the slope in the inertial subrange never quite reaches -5/3, which is fairly consistent with the velocity measurements of Mydlarski and Warhaft (1996). Similarly, measurements of reactant concentrations in near isothermal turbulent reactive flows typically display PSDs with a slope in the inertial-convective region near -5/3 (Li et al., 1993), although slopes closer to -3.0 were observed by Masutani and Bowman (1986) for a two-dimensional shear layer. In a flame, however, the relationship between velocity and scalar fluctuations becomes much more complicated as compared to near-isothermal flows. In particular, many scalar profiles become very sharp with respect to location in the flame. This feature causes fluctuations in the scalar to be strongly affected by convection since rather small velocity fluctuations could cause large scalar fluctuations. Moreover, the existence of non-uniform scalar distributions throughout the flow probably makes fluctuations originating from any convective source quite non-isotropic.

This difficulty is demonstrated by temperature PSDs measured via compensated fine-wire thermocouples in a turbulent C_3H_8/air diffusion flame by McQuay and Cannon (1996). For all measured locations in the flame, the PSDs are found to decay with slopes steeper than -2.0. Similar results are reported for temperature PSDs obtained via Rayleigh scattering in a CH_4/H_2 diffusion flame by Dibble and Hollenbach (1981). In both studies, the associated PDFs are observed to be not quite bimodal and highly asymmetric. Similarly, the early hydroxyl PSDs reported by Renfro et al. (1998) are observed to decay with slopes steeper than -2.0 at all locations for which the hydroxyl PDF is bimodal. This behavior is consistent with turbulent PDF analysis (Peters, 1986); moreover, both the steep PSD slope and the bimodal PDF shape can be derived from the species conservation equation if all fluorescence fluctuations are assumed to arise from convection (Renfro et al., 1998). On the other hand, for locations where the PDF is Gaussian, the high-frequency slope of the hydroxyl PSDs is around -1.2 in most cases. This slope is insufficiently steep to be described solely by convection. The associated regions are low in the turbulent diffusion flame where the flame is attached to the burner. In these regions, the scalar dissipation rate is much higher (Effelsberg and Peters, 1988) and neglecting source terms when evaluating the influence of fluctuating species concentrations likely becomes invalid. In particular, the PSDs for other species and for temperature may need to be considered to calculate reaction rates and thus describe hydroxyl PSDs in such regions.

Recall that the integral scale for turbulent fluctuations is defined as the temporal integral of the autocorrelation function. As this function is simply the Fourier transform pair of the PSD, the integral time scale for OH fluctuations may be computed by simply integrating the Fourier transform of each shot-noise corrected PSD shown in Fig. 13. A plot of these integral time scales is shown in Fig. 14. Note that the integral time scale for OH fluctuations is inversely proportional to the Reynolds number, as might be expected for passive scalars which are dominated by convective transport. While the latter condition is not necessarily characteristic of reactive scalars, it is not entirely surprising in this case owing to the applicability of the conserved scalar hypothesis for hydroxyl in H_2/Ar flames (Renfro et al., 1999c). In fact, the influence of the Reynolds number may be directly observed by instead employing normalized power spectra.

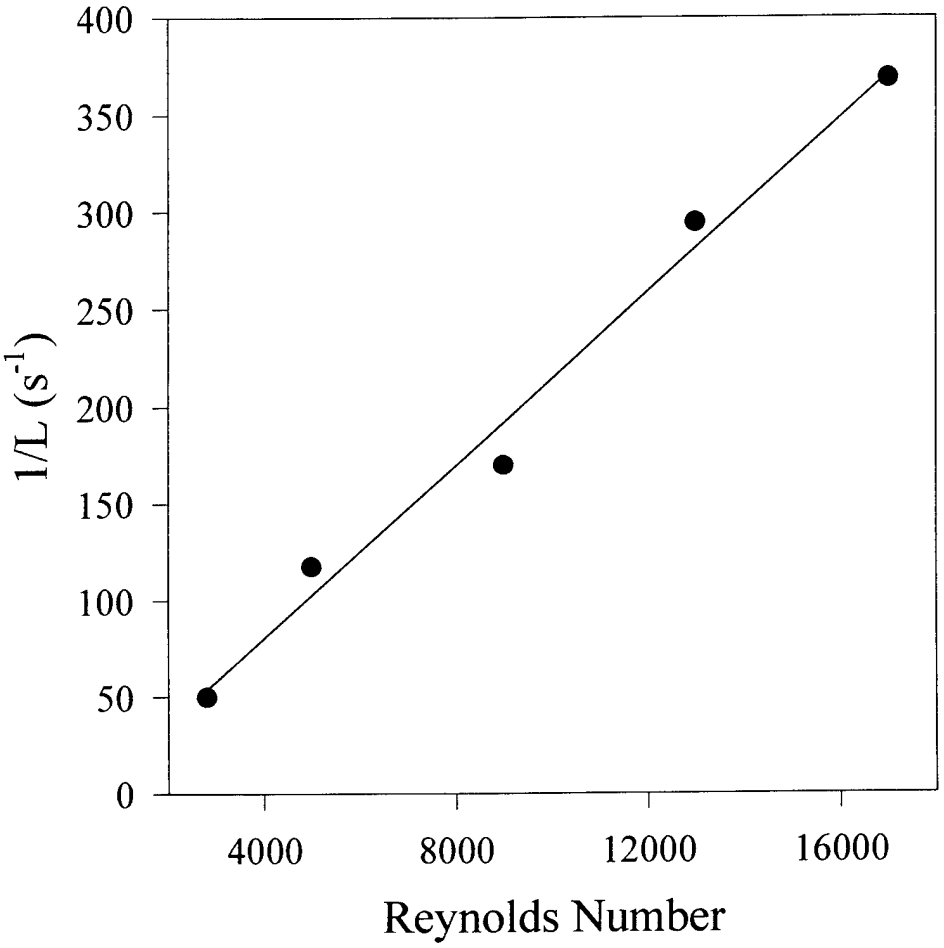

Figure 14. Inverse integral time scale computed from the Fourier transform of the shot-noise-corrected PSDs of hydroxyl concentration from Fig. 13.

Figure 15 shows the same PSDs as in Fig. 13, but with the frequency multiplied by the integral scales from Fig. 14, which is obviously equivalent to dividing by the Reynolds number. We note that the measured hydroxyl PSDs collapse almost perfectly onto a single normalized spectrum. Hence, as expected, OH concentrations in H_2/Ar flames are generally well described by the laminar flamelet approximation.

3 CONCLUSIONS

In summary, a novel integrated photon-counting technique has been developed which combines four simultaneous measurements to determine the fluorescence signal, fluorescence lifetime, and flame emission background for OH in turbulent flames. The sampling rate and memory depth of the electronics used in the implementation of this technique have permitted time-series measurements of these quantities so as to determine temporal fluctuations of minor-species concentrations. Quantitative time-series measurements of hydroxyl concentrations have been obtained in a series of turbulent H_2/Ar/air nonpremixed flames. These are the first time-series measurements for any minor species which directly account for fluctuations in the fluorescence quantum yield.

The major conclusions relevant to this report can be summarized as follows.

(1) Simultaneous OH fluorescence and lifetime measurements can now be made with a precision better than 10% at sampling rates up to 4 kHz. Hence, concentration time-series measurements can be obtained with sufficient spatial and temporal resolution to permit detailed, quantitative investigations of concentration PSDs and PDFs in turbulent nonpremixed flames. The current instrument is appropriate for radical species with fluorescence lifetimes in the 1.5-3.0 ns range. Hence, PITLIF can be applied to any species meeting this requirement for which the laser system can be tuned to access appropriate rovibronic transitions.

(2) For the turbulent flames investigated thus far, the influence of lifetime fluctuations on hydroxyl PSDs is negligible. Given confirmation of this result at each measurement location, fluorescence PSDs can be interpreted as concentration PSDs. This feature permits an improvement of the bandwidth for measured PSDs. However, the insensitivity of PSDs to fluorescence lifetime will not necessarily hold for all species and thus lifetime corrections must be examined for other species such as NO.

(3) An analysis of the hydroxyl PSDs shows a remarkable collapse for Re = 2800-17,000 in H_2/Ar flames when the PSD frequency is normalized by the integral time scale. While such a collapse would be expected for both velocity and passive scalars in a nonreacting jet, it appears unlikely in reacting jets unless a robust state relationship exists between OH concentration and the local mixture fraction. Such a relationship is assumed by the laminar flamelet model; thus, the present results suggest that a similar relationship must exist in advanced combustion models.

Although minor-species PSDs are now accessible via PITLIF, comparisons to previous investigations are severely limited by the paucity of available information in the literature. In particular, while a large body of work exists on the temporal behavior of velocity fields in turbulent nonreacting flows (Tennekes and Lumley, 1972; Mydlarski and Warhaft, 1996), little spectral information is available on either velocity or scalar fields in reacting flows. Masutani and Bowman (1986) and Li *et al.* (1993) have examined reactant concentrations and other scalar spectra only for near-isothermal shear flows. Gökalp *et al.* (1988) have addressed the effects of flame heat release on velocity spectra, but the equally important effects on scalar spectra have

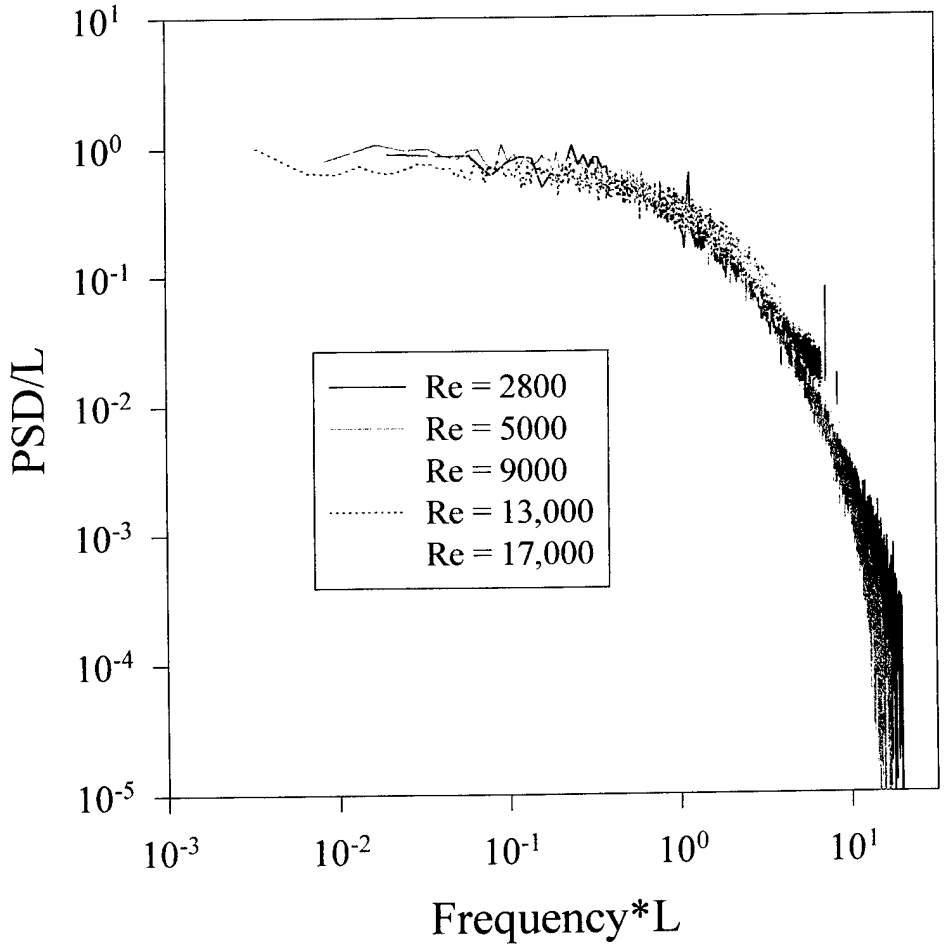

Figure 15. Normalized hydroxyl power spectra from Fig. 13. Each spectrum was individually normalized by using the appropriate integral scale from Fig. 14.

scarcely received any attention (McQuay and Cannon, 1996; Kounalakis *et al.,* 1988). Consequently, the advent of PITLIF clearly presents a new opportunity to understand more completely the influence of heat release and velocity fluctuations on radical species in turbulent flames. Such a study of radical concentration spectra, which is currently nonexistent, would clearly supplement existing measurements for other scalars and could provide a novel means for direct investigation of controlling turbulence-chemistry interactions in practical flame systems.

4 REFERENCES

Ballew, R.M. and Demas, J.N. (1989), *Anal. Chem.* **61**, 30.

Barlow, R.S. and Carter, C.D. (1994), *Combust. Flame* **97**, 261.

Bowman, C.T., Hanson, R.K., Davidson, D.F., Gardiner Jr., W.C., Lissianski, V., Smith, G.P., Golden, D.M., Frenklach, M., and Goldenburg, M., http://www.me.berkley.edu/gri_mech/ (1995).

Box, G. E. P. and Jenkins, G. M. (1976), *Time Series Analysis*, Holden-Day, San Francisco.

Daily, J.W. (1976), *Appl. Opt.* **15**, 955.

Dibble, R.W., and Hollenbach, R.E. (1981), *Eighteenth Symposium (International) on Combustion*, The Combustion Institute, Pittsburgh, pp. 1489-1499.

Drake, M.C. and Pitz, R.W. (1985), *Exp. Fluids* **3,** 283.

Effelsberg, E., and Peters, N. (1998), *Twenty-second Symposium (International) on Combustion*, The Combustion Institute, Pittsburgh, pp. 693-700.

Gaskey, S., Vacus, P., David, R., Villermaux, J., and André, J.C. (1990), *Exp. In Fluids* **9**, 137.

Gökalp, I., Shepherd, I.G., and Cheng, R.K. (1988), *Combust. Flame* **71**, 313.

Kee, R.J., Grcar, J.F., Smooke, M.D., and Miller, J.A. (1985), Sandia National Laboratory, SAND85-8240.

Kounalakis, M.E., Gore, J.P., and Faeth, G.M. (1991), *J. Heat Trans.* **113**, 437.

Lampert, R.A., Chewter, L.A., Phillips, D., O'Connor, D.V., Roberts, A.J., and Meech, S.R. (1983), *Anal. Chem.* **55**, 68.

Li, J.D., Brown, R.J., and Bilger, R.W. (1993), *Turbulent Shear Flows* **9**, Springer-Verlag, Berlin, pp. 411-425.

Lutz, A.E., Kee, R.J., and Grcar, J.F. (1996), Sandia National Laboratory, SAND96-8243.

Masutani, S.M., and Bowman, C.T. (1986), *J. Fluid Mechanics* **172**, 93.

McQuay, M.Q., and Cannon, S.M. (1996), *Combust. Sci. and Technol.* **119**, 13.

Miller, P. L., and Dimotakis, P. E. (1996), *J. Fluid Mech.* **308**, 129.

Mydlarski, L., and Warhaft, Z. (1996), *J. Fluid Mech.* **320,** 331.

O'Conner, D.V., Meech, S.R., and Phillips, D. (1982), *Chem. Phys. Lett.* **88**, 22.

O'Conner, D.V. and Phillips, D. (1984), *Time-correlated Single Photon Counting*, Academic Press, New York .

Pack, S.D., Renfro, M.W., King, G.B., and Laurendeau N.M. (1998), *Opt. Lett.* **23**, 1215.

Pack, S.D., Renfro, M.W., King, G.B., and Laurendeau, N.M. (1999), *Combust. Sci. Technol.* **140**, 405.

Peters, N., *Twenty-first Symposium (International) on Combustion* (1986), The Combustion Institute, Pittsburgh, pp. 1231-1250.

Ravikrishna, R.V., and Laurendeau, N.M. (1998), *Combust. Flame* **113**, 473.

Reichardt, T.A., Klassen, M.S., King, G.B., and Laurendeau, N.M. (1995), *Appl. Opt.* **34**, 973.

Reichardt, T.A., Klassen, M.S., King, G.B., and Laurendeau, N.M. (1996), *Appl. Opt.* **35**, 2125.
Reisel, J.R., Carter, C.D., and Laurendeau, N.M. (1997), *Energy and Fuels* **11**, 1092.
Renfro, M.W., Pack, S.D., King, G.B., and Laurendeau, N.M. (1998), *Combust. Flame* **115**, 443.
Renfro, M.W., Pack, S.D., King, G.B., and Laurendeau, N.M. (1999a), *Appl. Phys. B* **69**, 137.
Renfro, M.W., King, G.B., and Laurendeau, N.M. (1999b), *Appl. Opt.* **38**, 4596.
Renfro, M.W., Sivathanu, Y.R., Gore, J.P., King, G.B., and Laurendeau, N.M. (1999c), *Twenty-seventh Symposium (International) on Combustion,* Boulder, Colorado.
Tennekes, H., and Lumley, J.L. (1972), *A First Course in Turbulence*, The MIT Press, Cambridge, MA.

5 RELATED PUBLICATIONS AND PRESENTATIONS

Pack, S. D., Renfro, M. W., King, G. B., and Laurendeau, N. M. (1998). Photon-counting technique for rapid fluorescence decay measurements. *Optics Letters*, v. 23, 1215-1217.

Pack, S. D., Renfro, M. W., King, G. B., and Laurendeau, N. M. (1998). Laser-induced fluorescence triple-integration method applied to hydroxyl concentration and fluorescence lifetime measurements. *Combustion Science and Technology*, v. 140, 405-425.

Renfro, M. W., Sivathanu, Y. R., Gore, J. P., King, G. B., and Laurendeau, N. M. (1998). Time-series analysis and measurements of intermediate species concentration spectra in turbulent nonpremixed flames. *Twenty-Seventh Symposium (International) on Combustion*, The Combustion Institute, Pittsburgh, PA, 1015-1022.

Renfro, M. W., Pack, S. D., King, G. B., and Laurendeau, N. M. (1999). A pulse-pileup correction procedure for rapid measurements of hydroxyl concentrations using picosecond time-resolved laser-induced fluorescence. *Applied Physics B*, v. 69, 137-146.

Renfro, M. W., King, G. B., and Laurendeau, N. M. (1999). Quantitative hydroxyl-concentration time-series measurements in turbulent nonpremixed flames. *Applied Optics*, v. 38, 4596-4608.

Pack, S. D., Renfro, M. W., King, G. B., and Laurendeau, N. M. (1998). Photon-counting technique for rapid fluorescence decay measurements, Proceedings of the Central States Section Meeting, The Combustion Institute, Lexington, KY.

Renfro, M. W., Sivathanu, Y. R., Gore, J. P., King, G. B., and Laurendeau, N. M. (1998). Time-series analysis and measurements of intermediate species concentration spectra in turbulent nonpremixed flames. Proceedings of the Central States Section Meeting, The Combustion Institute, Lexington, KY.

Renfro, M. W., Pack, S. D., King, G. B., and Laurendeau, N. M. (1998). Quantitative hydroxyl-concentration time-series measurements in turbulent nonpremixed flames. *Third International Workshop on Turbulent Nonpremixed Flames*, Boulder, CO.

Renfro, M. W., Pack, S. D., King, G. B., and Laurendeau, N. M. (1998). A new photon-counting technique for rapid, quantitative hydroxyl-concentration time-series measurements. *Twenty-Seventh Symposium (International) on Combustion*, Boulder, CO.

Renfro, M. W., King, G. B., and Laurendeau, N. M. (1999). Quantitative hydroxyl-concentration time-series measurements in turbulent diffusion flames. Proceedings of the Joint U.S. Sections Meeting, The Combustion Institute, Washington, D.C.

Renfro, M. W., King, G. B., and Laurendeau, N. M. (1999). Time-series measurements of OH and CH in turbulent nonpremixed flames. *Gordon Research Conference on The Physics and Chemistry of Laser Diagnostics in Combustion*, Barga, Italy.

Renfro, M. W., Pack, S. D., King, G. B., and Laurendeau, N. M. (1999). Time-series measurements of minor-species concentrations in turbulent flames via picosecond time-resolved laser-induced fluorescence. Presented at the Annual Meeting, The Optical Society of America, Santa Clara, CA.

AUGMENTATION AWARDS FOR SCIENCE & ENGINEERING RESEARCH TRAINING (AASERT) REPORTING FORM

The Department of Defense (DoD) requires certain information to evaluate the effectiveness of the AASERT Program. By accepting this Grant which bestows the AASERT funds, the Grantee agrees to provide 1) a brief (not to exceed one page) narrative technical report of the research training activities of the AASERT-funded student(s) and 2) the information requested below. This information should be provided to the Government's technical point of contact by each annual anniversary of the AASERT award date.

1. Grantee identification data: (R&T and Grant numbers found on Page 1 of Grant)

a. Purdue University
University Name

b. F49620-96-1-0272
Grant Number

c. _____
R&T Number

Galen B. King

d. Normand M. Laurendeau
P.I. Name

e. From: 6/15/96 To: 12/31/99
AASERT Reporting Period

NOTE: Grant to which AASERT award is attached is referred to hereafter as "Parent Agreement".

2. Total funding of the Parent Agreement and the number of full-time equivalent graduate students (FTEGS) supported by the Parent Agreement during the 12-month period prior to the AASERT award date.

a. Funding: $ 130,763

b. Number FTEGS: 1

3. Total funding of the Parent Agreement and the number of FTEGS supported by the Parent Agreement during the current 12-month reporting period.

a. Funding: $ 138,108

b. Number FTEGS: 1

4. Total AASERT funding and the number of FTEGS and undergraduate students (UGS) supported by AASERT funds during the current 12-month reporting period.

a. Funding: $ 39,300

b. Number FTEGS: 1

c. Number UGS: 0

VERIFICATION STATEMENT: I hereby verify that all students supported by the AASERT award are U.S. citizens.

Galen B. King
Principal Investigator

January 24, 2000
Date

Principal Investigator Annual Data Collection (PIADC) Survey Form

Please submit the requested data for the period 1 October 199 through 30 September 199 . Request you follow the data requirements and format instructions below. This data is due to your AFOSR program manager NLT 30 September 199

NOTE: If there is insufficient space on this survey to meet your data submissions, please submit additional data in the same format as identified below.

PI DATA

Name (Last, First, MI): King, Galen B.
Laurendeau, Normand M.

Institution: Purdue University

Contract/Grant No.: F49620-96-1-0272

AFOSR USE ONLY
Project/Subarea
_____/____

NX _____

FY _____

NUMBER OF CONTRACT/GRANT CO-INVESTIGATORS

Faculty 2 Post Doctorates_____ Graduate Students 1 Other_____

PUBLICATIONS RELATED TO AFOREMENTIONED CONTRACT/GRANT

NOTE: List names in the following format: Last Name, First Name, MI

Include: Articles in peer reviewed publications, journals, book chapters, and editorships of books.

Do Not Include: Unreviewed proceedings and reports, abstracts, "Scientific American" type articles, or articles that are not primary reports of new data, and articles submitted or accepted for publication, but with a publication date outside the stated time frame.

Name of Journal, Book, etc.: Applied Optics

Title of Article: Quantitative hydroxyl-concentration time-series measurements in turbulent nonpremixed flames

Author(s): M.W. Renfro, G.B. King and N.M. Laurendeau

Publisher (if applicable): _____

Volume: 38 Page(s): 4596-4608 Month Published: _____ Year Published: 1999

Name of Journal, Book, etc.: _____

Title of Article: _____

Author(s): _____

Publisher (if applicable): _____

Volume: _____ Page(s): _____ Month Published: _____ Year Published: _____